ARCHIVES OF ELECTRICAL ENGINEERING VOL. 70(4), pp. 759–775 (2021)

DOI 10.24425/aee.2021.138259

Design of a Taguchi-GRA optimized PID and adaptive PID controllers for speed control of DC motor

MARY ANN GEORGE, DATTAGURU V. KAMAT

Department of Electronics and Communication Engineering
Manipal Institute of Technology, Manipal Academy of Higher Education (MAHE)
Manipal – 576104, Udupi District, Karnataka State, India
e-mail: {starmaryann1247/reachdvkamath}@yahoo.com, dv.kamath@manipal.edu

(Received: 29.10.2020, revised: 19.04.2021)

Abstract: DC motors have wide acceptance in industries due to their high efficiency, low costs, and flexibility. The paper presents the unique design concept of a multi-objective optimized proportional-integral-derivative (PID) controller and Model Reference Adaptive Control (MRAC) based controllers for effective speed control of the DC motor system. The study aims to optimize PID parameters for speed control of a DC motor, emphasizing minimizing both settling time (T_s) and % overshoot (% OS) of the closed-loop response. The PID controller is designed using the Ziegler Nichols (ZN) method primarily subjected to Taguchi-grey relational analysis to handle multiple quality characteristics. Here, the Taguchi L9 orthogonal array is defined to find the process parameters that affect T_s and % OS. The analysis of variance shows that the most significant factor affecting T_s and % OS is the derivative gain term. The result also demonstrates that the proposed Taguchi-GRA optimized controller reduces T_s and % OS drastically compared to the ZN-tuned PID controller. This study also uses MRAC schemes using the MIT rule, Lyapunov rule, and a modified MIT rule. The DC motor speed tracking performance is analyzed by varying the adaptation gain and reference signal amplitude. The results also revealed that the proposed MRAC schemes provide desired closed-loop performance in real-time in the presence of disturbance and varying plant parameters. The study provides additional insights into using a modified MIT rule and the Lyapunov rule in protecting the response from signal amplitude dependence and the assurance of a stable adaptive controller, respectively.

Key words: analysis of variance, Lyapunov rule, MIT rule, model reference adaptive control, Taguchi-grey relational analysis

1. Introduction

DC motors have gained popularity over induction motors and brushless DC motors due to their several advantages: easy control, high electromagnetic torque, and wide range speed adjustment [1]. DC motors are extensively used in commercial and industrial applications like robotics, mechatronic systems, electric vehicles, disk drive, mining, and construction [2]. Hence, improving the quality of its control is significant to avoid machine damage. Although various control schemes are used in DC motor control [3–5], the PID controllers are widely used in speed control applications due to their simplicity, flexibility in tuning, and implementation [6–8]. However, these controllers cannot handle disturbance and parameter variations. To overcome these problems, adaptive control strategies like the model reference adaptive control (MRAC) based PID controller has been introduced for better performance and accuracy. The tuning of the PID controller can be by using the Ziegler Nichols (ZN) method, Cohen Coon method, approximate M-constrained integral gain optimization (AMIGO method) [9, 10], which can give an initial estimate of controller parameters. Multi-objective optimization plays a significant role when there are two conflicting objectives: to minimize the settling time (T_s) and % overshoot (% OS) of the closed-loop DC motor speed control response. The genetic algorithm [11], ant colony optimization [12], particle swarm optimization [13] are some of the PID multi-objective optimization methods.

Design of experiments (DOE) is an effective method for assessing process parameters' effects on the process characteristics and finding the optimum process parameters. The Taguchi method is a powerful DOE technique to provide a systematic means to optimize the process. Although the Taguchi method is a single objective optimization method used to optimize multi-parameter combination with a few numbers of experiments, its combination with grey relational analysis (GRA) makes it a multi-objective optimization method [14, 15].

MRAC is an effective adaptive control scheme that can deal with parameter changes, uncertainties, and disturbances. This scheme was extensively used in aerospace engineering, as the controller does not rely on the plant's accurate model. The MRAC scheme's performance for speed tracking of a brushless DC motor is found to be superior to the fuzzy-based PID controller regardless of the presence of parameter uncertainties and disturbances [16]. Neogi B. *et al*. [17] presented an MRAC scheme using the gradient method for mechanical prosthetic arm control. The Lyapunov rule, which is a generalized and stable rule, was also introduced. Both schemes could handle disturbances and parameter variations. Although the MRAC scheme using the Massachusetts Institute of Technology (MIT) rule is widely used in applications like speed control of a DC motor [18], inverted pendulum [19], the major drawback of this scheme is that the tracking response can become oscillatory and unstable when the reference signal input increases. A modified MIT rule called the normalized algorithm is insensitive to reference signal changes and stable [20].

Having noted the importance of control schemes to handle parameter variation and disturbance in DC motor speed control, this work introduces a multi-objective optimized PID controller and MRAC schemes for motor control. The main objective is to design a PID controller for a DC motor using the ZN method and perform Taguchi-GRA to obtain optimum PID parameter combination. Next, the PID controller designed is appended with adaptive rules like the MIT rule, a modified MIT rule, and the Lyapunov rule. The outcome thus produced may be beneficial to many industrial applications using DC motor control.

The paper is organized as follows: Section 2 describes the DC motor mathematical modeling. Section 3 explains the Taguchi-GRA for multi-objective optimization. MRAC schemes using the MIT rule, a modified MIT rule, and the Lyapunov rule are discussed in Section 4. Section 5 presents the simulation results and inferences. Finally, Section 6 summarizes the findings and concluding remarks.

2. DC motor mathematical modelling

DC motors are standard actuators in the control system that converts electrical energy to rotational mechanical energy and are widely used in industrial applications [21, 22].

Figure 1 shows the DC motor's electrical equivalent circuit showing an armature circuit and a free-body diagram of the rotor. The DC motor parameters and specifications are given in [23].

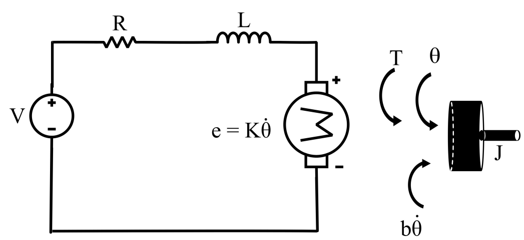

Fig. 1. Electrical equivalent circuit of DC motor

The armature voltage V and rotational speed of the shaft $\dot{\theta}$ are the input and output of the DC motor speed control system, respectively. The motor torque T is related to the armature current i, and the back emf E is related to the angular velocity $\dot{\theta}$.

$$T = K_t i \qquad \text{and} \qquad E = K_e \dot{\theta}. \tag{1}$$

Also

$$K_e = K_t = K, \tag{2}$$

where K_e denotes the back emf constant and K_t represents the torque constant. By using Newton's second law of motion and Kirchhoff's voltage law in Fig. 1, the following equations are obtained.

$$J\ddot{\theta} + b\dot{\theta} = Ki, \tag{3a}$$

$$L\frac{\mathrm{d}i}{\mathrm{d}t} + Ri = V - K\dot{\theta}, \tag{3b}$$

where: R is the electrical resistance, L is the electrical inductance, b is the viscous friction coefficient, and J is the moment of inertia of the rotor. Figure 2 shows the block diagram representation of the DC motor. Applying the Laplace transform to (3a) and (3b) and further simplification the transfer function of DC motor speed takes the form:

$$\frac{\dot{\theta}(s)}{V(s)} = \frac{(K/JL)}{s^2 + s\left(\dfrac{R}{L} + \dfrac{b}{J}\right) + \dfrac{\left(K^2 + bR\right)}{JL}} = \frac{19649}{(s + 162.2)(s + 38.7)}\ \frac{\text{rad/sec}}{\text{V}}\,. \tag{4}$$

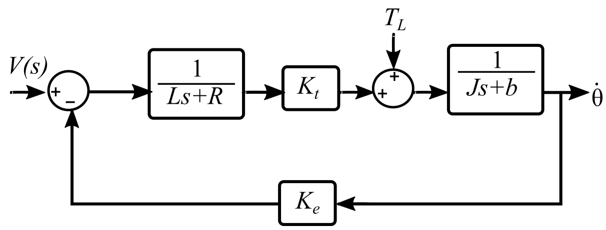

Fig. 2. Block diagram of DC motor

3. Taguchi-grey relational analysis (Taguchi-GRA)

The Taguchi method is generally a single objective optimization method, which uses an orthogonal array to plan out the experiment and analyze the data obtained from the experiment using a signal-to-noise (S/N) ratio. The orthogonal array reduces variance and the number of experiments to be conducted. The Taguchi method uses an L9 orthogonal array with nine experiments if there are three control factors and three levels. An S/N ratio measures the robustness of the process and finds its deviation from the desired values. A higher S/N ratio is preferred as this can reduce the noise and effect of uncontrollable factors. There are three types of S/N ratios, i.e., higher-the-better (HTB), nominal-the-better (NTB), and smaller-the-better (STB). In this work, the S/N ratio is calculated by STB and is given by

$$\left(\frac{S}{N}\right)_{\text{STB}} = -10\log_{10}\left(\frac{1}{n}\sum_{j=1}^{n} x_j^2\right), \tag{5}$$

where n is the number of experiments and x_j is the response value of the j-th experiment in the orthogonal array.

The PID controller is designed for the DC motor system given in (4) using the ZN method. The transfer function of the PID controller obtained is given by

$$C_{\text{PID}}(s) = 2.2 + \frac{232.04}{s} + 0.005s. \tag{6}$$

Table 1 shows the three control factors K_p, K_i, and K_d at three levels used to evaluate the DC motor system's speed tracking performance. Table 2 presents the Taguchi L_9 orthogonal

Table 1. PID controller parameter values at 3 levels

Control factors	**Levels**		
	1	**2**	**3**
Proportional gain K_p	1.8	2.2	2.6
Integral gain K_i	228	232	236
Derivative gain K_d	0.002	0.005	0.008

array designed with nine runs. The DC motor speed tracking performance is assessed using two response variables, i.e., T_s and % OS. As lower values of settling time and % overshoot are preferred, STB quality characteristic is selected. The S/N ratio can be calculated from (5) using Minitab 15 statistical software. Here, the effect of varying the control factor K_p, K_i, and K_d on T_s and % OS is analyzed.

Table 2. Taguchi orthogonal array with S/N ratios of T_s and % OS

Run	Control factors			Response values		S/N ratio (dB)	
	K_p	K_i	K_d	T_s (sec)	% OS	T_s	% OS
1	1.8	228	0.002	0.082	43.8	21.724	–32.829
2	1.8	232	0.005	0.071	33.1	22.975	–30.397
3	1.8	236	0.008	0.075	25.6	22.499	–28.165
4	2.2	228	0.005	0.047	28.5	26.558	–29.097
5	2.2	232	0.008	0.052	20.9	25.679	–26.403
6	2.2	236	0.002	0.071	43.0	22.975	–32.669
7	2.6	228	0.008	0.043	19.2	27.331	–25.666
8	2.6	232	0.002	0.053	40.2	25.514	–32.085
9	2.6	236	0.005	0.042	28.4	27.535	–29.066

The grey relation analysis (GRA) combined with the Taguchi method is used for multiple response analyses. This combination helps find the optimum PID parameter combination when several conflicting objectives are met simultaneously. The following are steps involved in GRA analysis:

a. Normalize the reference sequence within the range of zero and one by

$$y_j^*(k) = \frac{\max\left(x_j(k)\right) - x_j(k)}{\max\left(x_j(k)\right) - \min\left(x_j(k)\right)}, \tag{7}$$

where $x_j(k)$ is the initial sequence of the mean of the responses and $y_j^*(k)$ is the comparability sequence.

b. Calculate the deviation sequence of the reference sequence by

$$\Delta_{0j} = \left|y_0^*(k) - y_j^*(k)\right|, \tag{8}$$

where $y_0^*(k)$ is the reference sequence.

c. Compute the grey relational coefficient (GRC) $\xi_j(k)$ by

$$\xi_j(k) = \frac{\Delta_{\min} + \zeta\Delta_{\max}}{\Delta_{0j}(k) + \zeta\Delta_{\max}}, \tag{9}$$

where: $\Delta_{\max}$ is the maximum deviation of each response variable, $\Delta_{\min}$ is the minimum deviation of each response variable, Δ_{0j} is the deviation sequence and $\zeta \in [0, 1]$ is the identification coefficient which takes the value equal to 0.5.

d. Compute the grey relational grade (GRG) by averaging the GRC of each response variable.

$$\gamma_j = \frac{1}{n}\sum_{j=1}^{n} \xi_j(k), \tag{10}$$

where n is the aggregate count of the performance characteristics and γ_j is the GRG for the j-th experiment.

e. Predict and verify the quality characteristics by

$$\gamma_{\text{predicted}} = \gamma_m + \sum_{j=1}^{q} \gamma_0 - \gamma_m\,, \tag{11}$$

where: γ_m is the mean of the GRG, γ_0 represents the maximum of average GRG at the optimum level of factors, and the quantity q represents the number of factors.

4. Model reference adaptive control (MRAC) scheme

MRAC is an essential adaptive control method developed in Draper Laboratory at the Massachusetts Institute of Technology (MIT) [24]. The MRAC scheme offers good tracking capability and robust performance to the plant with parameter uncertainties. The MRAC scheme comprises a linear or non-linear plant with uncertainty, reference model, controller, and adaptive law. The controller gains are updated based on the plant output and reference model output, such that the plant-model error is close to zero. In MRAC, high adaptation gain is preferred to achieve faster adaptation in the presence of uncertainties. However, this can introduce high-frequency oscillation in the system response, leading to instability of the system.

The adaptation mechanism can be based on the gradient method (the MIT rule) or applying stability theory (the Lyapunov rule). The reference model has the desired performance. Considering a closed-loop system with one adjustable parameter θ, and the MIT rule as an adaptation mechanism, the parameter θ is adjusted such that the cost function $J(\theta)$ is minimized.

$$J(\theta) = \frac{1}{2}e^2, \tag{12}$$

where e is the error between the plant and model output.

As the cost function related to the error must be minimized, it is reasonable to move in the negative gradient direction of J. Therefore, the MIT rule for the MRAC design is expressed as

$$\frac{\mathrm{d}\theta}{\mathrm{d}t} = -\gamma\frac{\delta J}{\delta\theta} = -\gamma e\frac{\delta e}{\delta\theta} = -\gamma y_m e, \tag{13}$$

where: $\frac{\delta e}{\delta\theta}$ is the sensitivity derivative, γ represents the adaptation gain and y_m denotes the model output. The reference model transfer function is obtained by carrying out closed-loop model identification by gathering reference input and plant output data. Similarly, the modified MIT rule or normalized algorithm is given by

$$\frac{\mathrm{d}\theta}{\mathrm{d}t} = \frac{-\gamma e\varphi}{\alpha + \varphi'\varphi}, \tag{14}$$

where $\varphi = \frac{\partial e}{\partial t}$ and $\alpha > 0$.

The Lyapunov rule is given by

$$\frac{\mathrm{d}\theta}{\mathrm{d}t} = -\gamma e u_c\,, \tag{15}$$

where u_c is the reference input.

The reference model is found by approximating the second-order DC motor transfer function in (4) to a first-order transfer function using 63% step response method [25], which is given by

$$G_1(s) = \frac{\dot{\theta}(s)}{V(s)} = \frac{3.12}{0.027s + 1}\ \frac{\text{rad/sec}}{\text{V}}\,. \tag{16}$$

Next, a PID controller is designed for the first-order system for zero percentage overshoot, zero steady-state error, and settling time less than 2 seconds.

$$C(s) = 0.1099 + \frac{5.837}{s}\,. \tag{17}$$

Hence, the reference model, which is the closed-loop transfer function of the first-order system and PI controller, is given by

$$R(s) = \frac{G_1(s)C(s)}{1 + G_1(s)C(s)} = \frac{12.75s + 676.67}{s^2 + 49.785s + 676.67}\,. \tag{18}$$

5. Simulation results and inference

This section describes the Taguchi-GRA optimized PID controller results for the speed control of the DC motor system. The Taguchi-GRA is carried out using Minitab 15 statistical software. Here, T_s and $\%\,OS$ are considered the two conflicting objective functions for optimization. An analysis of variance (ANOVA) is conducted to determine the influence of K_p, K_i, K_d on T_s, and $\%\,OS$ of the closed-loop response. This section also compares the speed tracking performance of an MRAC-based PID controller for a DC motor using the MIT rule, a modified MIT rule, and the Lyapunov rule.

5.1. Multi-objective optimized PID controller

The dominant control factors affecting T_s and $\%\,OS$ are identified from the response table shown in Table 3. It shows that K_p is the predominant control factor affecting T_s as the delta value is the highest. The next contributing factor is K_d, followed by K_i Similarly, K_d is the most influential factor affecting $\%\,OS$ with the highest value of delta. From Table 3, the desired factor levels, which can give a small value of T_s and a high value of an S/N ratio, are determined as K_p (level 3), K_i (level 1), and K_d (level 2). Similarly, K_p (level 3), K_i (level 1), and K_d (level 3) are the desired factor levels that can give a small value of $\%\,OS$.

ANOVA (shown in Table 4) is a way to determine the percentage contribution of each factor's effect on T_s and $\%\,OS$. ANOVA is conducted at a 95% confidence level, i.e., factors with a P-value less than 0.05 are considered significant. In the ANOVA table, the F ratio = adjacent mean square/adjacent mean Ssuare error. The high value of F indicates that the factor has a significant influence on the response variable. The Taguchi method generates two sets of optimal PID

Table 3. Response table for S/N ratio of T_s and % OS

	T_s			% OS		
Level	K_p	K_i	K_d	K_p	K_i	K_d
1	22.40	25.20	23.40	–30.46	–29.20	–32.53
2	25.07	24.72	25.69	–29.39	–29.63	–29.52
3	26.79	24.34	25.17	–28.94	–29.97	–26.74
Delta	4.39	0.87	2.28	1.52	0.77	5.78
Rank	1	3	2	2	3	1

parameter combinations for T_s and % OS. In practical applications, a single optimal PID parameter combination is required for both the response variables. Hence, GRA coupled with the Taguchi method solves the multi-response optimization problem with three control factors (K_p, K_i and K_d) and two response variables (T_s and % OS). The reference sequence and deviation sequence are calculated using (7) and (8), respectively.

Table 4. ANOVA for S/N ratio of T_s and % OS

Source	**DF**	**Adj SS**	**Adj MS**	**F**	**P**	**Contribution (%)**	**Remarks**
For T_s							
K_p	2	29.415	14.707	58.16	0.017	74.16	Significant
K_i	2	1.134	0.567	2.24	0.308	2.86	Not significant
K_d	2	8.608	4.304	17.02	0.055	21.70	Significant
Error	2	0.506	0.253				
Total	8	39.663					
For % OS							
K_p	2	3.681	1.840	19.93	0.048	6.69	Significant
K_i	2	0.892	0.446	4.83	0.172	1.62	Not significant
K_d	2	50.195	25.098	271.80	0.004	91.34	Significant
Error	2	0.185	0.092			0.34	
Total	8	54.953					

Table 5 presents the reference sequence and deviation sequence obtained after data pre-processing. Table 6 presents the GRCs and GRGs calculated using (9) and (10), respectively. The S/N ratios of the GRGs are also calculated. The 7th experiment run has the highest S/N ratio of GRC, and this is ranked one. Rank nine is assigned to the 1st experiment run. Once the ranks are assigned, the response table (shown in Table 7) is designed for the S/N ratio of the GRG.

Table 5. Reference and deviation sequence for GRA analysis

Run	**Reference sequence x_i^***		**Deviation sequence Δ_{0i}**	
	T_s	% OS	T_s	% OS
1	0.000	0.000	1.000	1.000
2	0.275	0.435	0.725	0.565
3	0.175	0.740	0.825	0.260
4	0.875	0.622	0.125	0.378
5	0.750	0.931	0.250	0.069
6	0.275	0.033	0.725	0.967
7	0.975	1.000	0.025	0.000
8	0.725	0.146	0.275	0.854
9	1.000	0.626	0.000	0.374

Table 6. GRCs, GRGs, and rank

Run	**GRC ε_i (*k*)**		**GRG γ_i**	**S/N ratio of GRG**	**Rank**
	T_s	% O_S			
1	0.333	0.333	0.333	–9.542	9
2	0.408	0.469	0.439	–7.154	7
3	0.377	0.658	0.518	–5.721	5
4	0.800	0.569	0.685	–3.289	4
5	0.667	0.879	0.773	–2.241	3
6	0.408	0.341	0.374	–8.532	8
7	0.952	1.000	0.976	–0.209	1
8	0.645	0.369	0.507	–5.895	6
9	1.000	0.572	0.786	–2.091	2

Table 7. Response table for S/N ratio of GRG

Level	K_p	K_i	K_d
1	–7.473	–4.347	–7.990
2	–4.688	–5.097	–4.178
3	–2.732	–5.448	–2.724
Delta	4.741	1.101	5.266
Rank	2	3	1

The GRG response table shows that K_d is the most significant factor influencing both T_s and % OS. The desired factor level, which can give minimum settling time and % overshoot, is determined as K_p (level 3), K_i (level 1), and K_d (level 3). ANOVA is conducted at a 95% confidence level for the S/N ratio of the GRG to find the significant and % percentage contribution of each control factor on T_s and % OS. Table 8 presents the ANOVA table for the GRG.

Table 8. ANOVA for S/N ratio of GRG

Source	DF	Adj SS	Adj MS	F	P	Contribution (%)	Remarks
K_p	2	34.055	17.027	49.98	0.020	42.04	Significant
K_i	2	1.897	0.949	2.78	0.264	2.34	Not significant
K_d	2	44.380	22.190	65.13	0.015	54.78	Significant
Error	2	0.681	0.341				
Total	8	81.013					

Considering the multiple responses of T_s and % OS, it is observed that K_d has the largest influence (54.78%) on the GRC, followed by K_p, with 42.04%, and K_i, with the minimum influence of 2.34%. Hence, the optimized PID controller parameter combination obtained from Taguchi-GRA is $K_p = 2.6$, $K_i = 228$, and $K_d = 0.008$. Figure 3 shows the DC motor system's closed-loop response using a ZN-tuned PID controller and Taguchi-GRA PID controller simulated in the MATLAB-Simulink environment. It shows that the settling time and % overshoot of the Taguchi-GRA tuned PID controller is smaller than the ZN-tuned PID controller for the DC motor system. This method can be used to fine-tune the PID parameters.

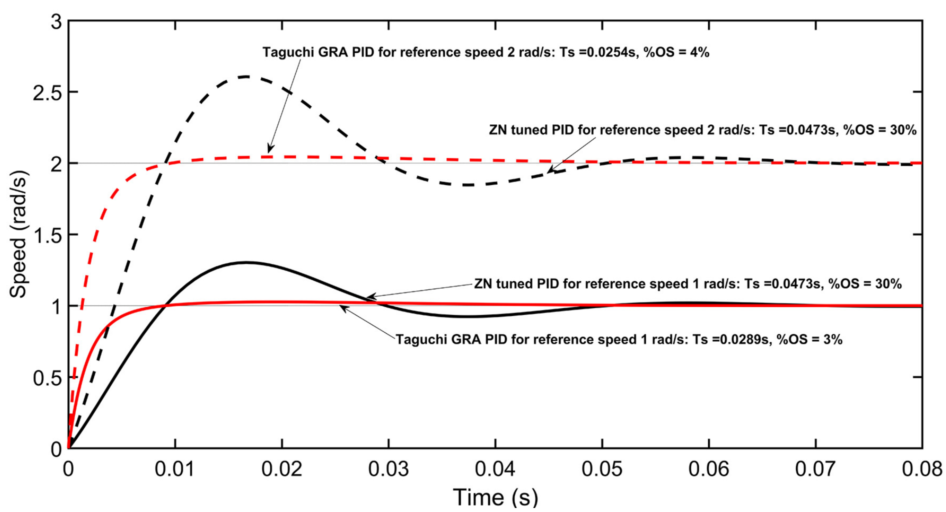

Fig. 3. Speed tracking response using ZN-tuned PID and Taguchi-GRA optimized PID for reference speed of 1 rad/s and 2 rad/s, respectively

5.2. MRAC based PID controller

Figure 4 shows the MRAC schemes for DC motor speed control using adaptive rules like the MIT rule, Lyapunov rule, and a modified MIT rule in the MATLAB Simulink environment.Figure 5 shows the plant output and reference model output for the MRAC based PID controller using the MIT rule by varying the adaptation gain γ. Here y_m is the model output, and y is the plant output for different values of γ. It indicates that as γ value increases, the settling time decreases and hence improves the tracking performance of the DC motor. In this work, γ is selected in the range $(0.5 < \gamma < 20)$, considering both the steady-state stability and transient response of the system.

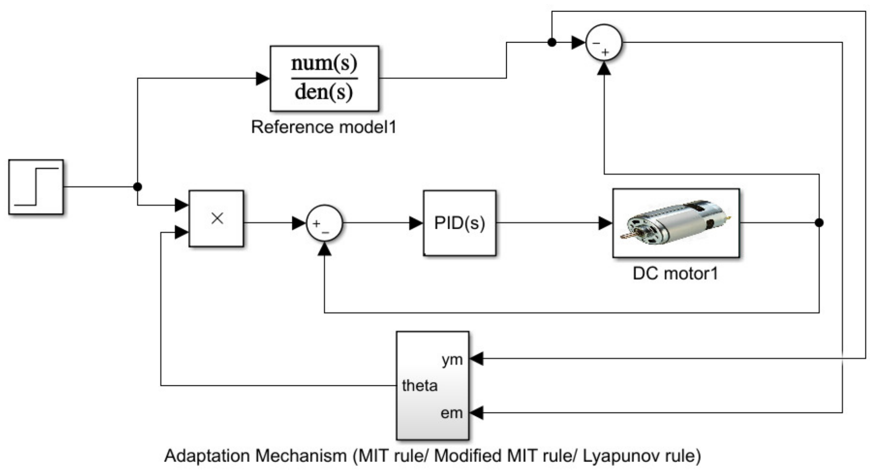

Fig. 4. MRAC based PID controller for DC motor speed control

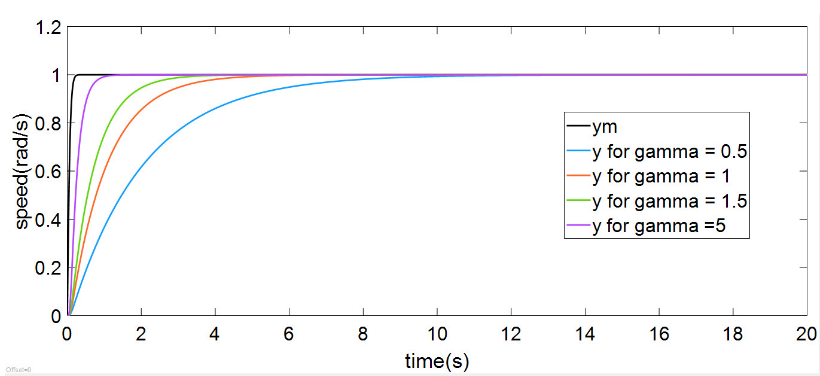

Fig. 5. Tracking performance of DC motor using MIT rule for different adaption gain γ

Table 9 shows the comparison of tracking the performance of a DC motor using the MIT rule, a modified MIT rule, and Lyapunov rule for a unit step input. It shows that the modified

Table 9. Effect of varying adaptation gain on the tracking performance of DC motor for a unit step input

Adaptation gain	Settling time (s) (2%)			Rise time (s)		
	MIT rule	Modified MIT rule	Lyapunov rule	MIT rule	Modified MIT rule	Lyapunov rule
0.5	7.952	7.878	7.936	4.281	4.210	4.301
1	3.971	3.932	3.945	2.129	2.150	2.129
1.5	2.663	2.620	2.638	1.414	1.427	1.414
5	0.837	0.781	0.799	0.424	0.420	0.424
10	0.447	0.407	0.411	0.223	0.222	0.225

MIT rule has the best tracking performance in terms of settling time, and the Lyapunov rule has a moderate performance. It also shows that the rise time decreases with the increase in adaptation gain. Next, the signal amplitude of reference input is varied, and adaptation gain is kept constant at 5. Figure 6 illustrates the tracking performance of a DC motor using the MIT rule for reference

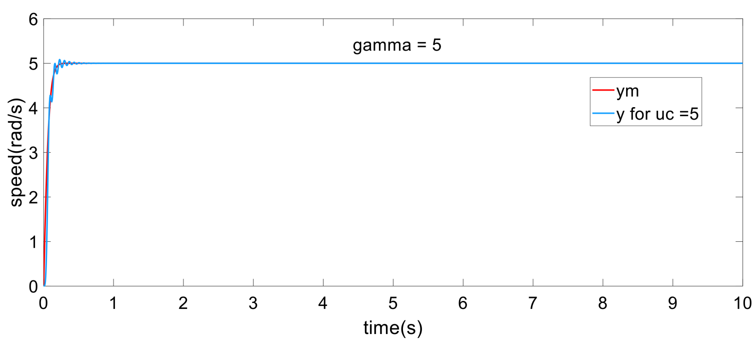

(a)

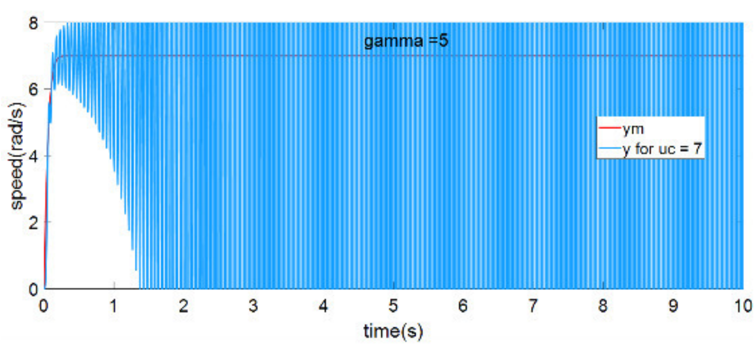

(b)

Fig. 6. Tracking performance of DC motor for varying reference signal amplitude using MIT rule: (a) $u_c = 5$; (b) $u_c = 7$

signal amplitudes $u_c = 5$ and 7. It is observed that the system becomes more sensitive and oscillatory for large values of reference signals while using the MIT rule. As this can lead to instability, a modified MIT rule is introduced.

Figure 7 shows the tracking performance of a DC motor using the modified MIT rule (alpha = 0.01) for reference input amplitude $u_c = 5$ and 7. Figure 7 demonstrates that the tracking performance using the modified MIT is insensitive to the reference signal amplitude and is stable.

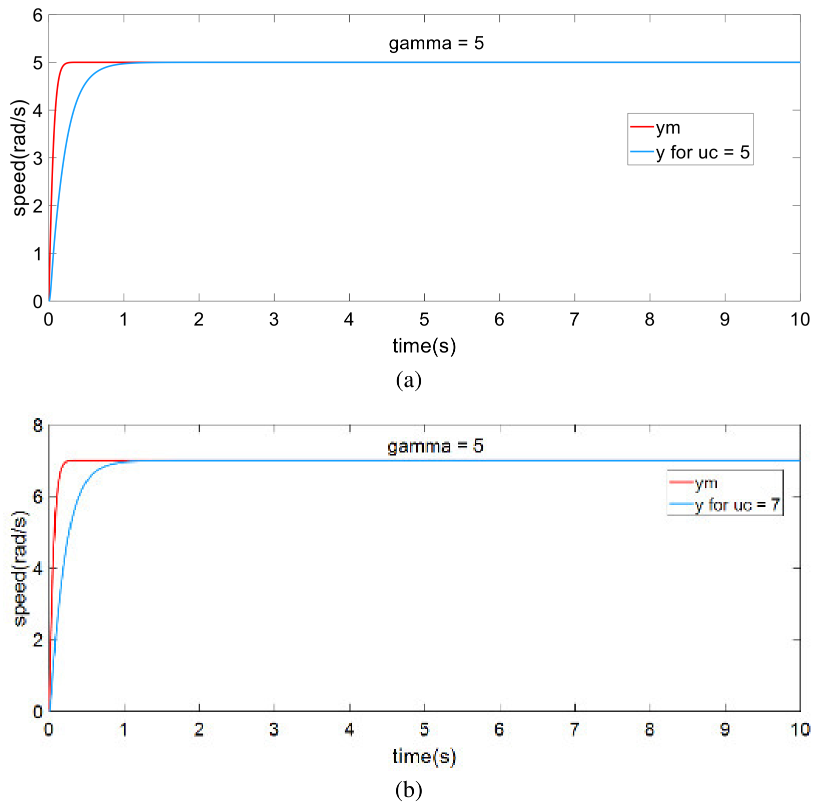

Fig. 7. Tracking performance of DC motor for varying reference signal amplitude using modified MIT rule: (a) $u_c = 5$; (b) $u_c = 7$

Next, the MRAC scheme is analyzed in the presence of disturbance. A step input with step time 3 s and a final value of 0.4 is the disturbance introduced in the DC motor control system. It is found that the MRAC scheme can handle disturbance and parameter variation with excellent tracking performance. Figure 8 shows the tracking performance of a DC motor using the MRAC scheme in the presence of disturbance.

Figure 9 shows a DC motor's tracking performance using the MIT rule, and the Lyapunov rule for a pulse train input. It is observed that the Lyapunov rule outperforms the MIT rule with a better time response with no excessive overshoot. The Lyapunov rule is a generalized rule to design a stable adaptive controller and can handle non-linear systems.

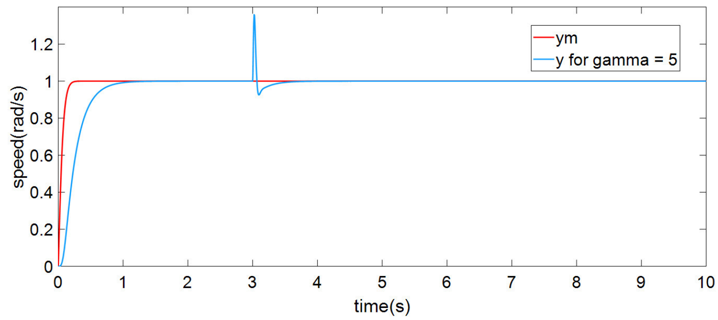

Fig. 8. Tracking performance of DC motor in the presence of disturbance

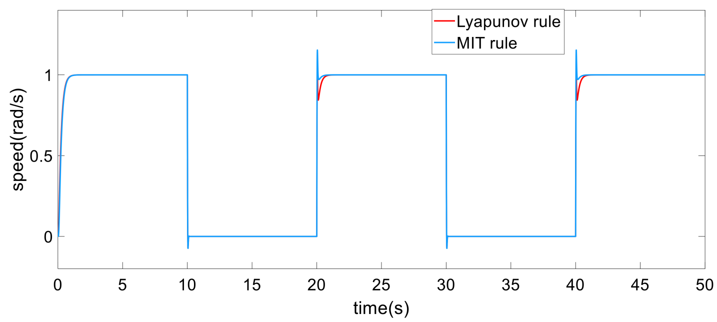

Fig. 9. Tracking performance of DC motor using MIT rule and Lyapunov rule for $\gamma = 5$ for a pulse train input

Finally, MRAC and Taguchi-GRA-based PID controllers' speed tracking performance is compared with the genetic algorithm (GA) and particle swarm optimization (PSO) based PID controllers, as illustrated in Fig. 10. Table 10 presents the time-domain performance of the DC

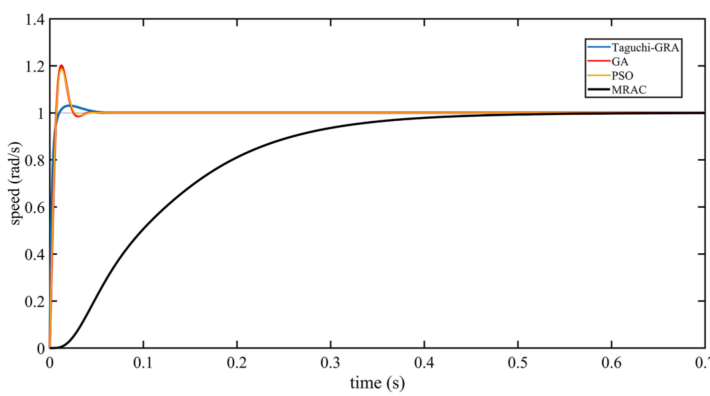

Fig. 10. Tracking performance of DC motor using various control schemes

motor using various control schemes. The parameters of optimization in [26] have been used in this work. It is observed that the Taguchi-GRA-based PID controller gives superior performance in terms of settling time and rise time as well as the MRAC based PID controller in terms of percentage overshoot.

Table 10. Comparison of various control schemes

Control schemes	Settling time (s) (2%)	Rise time (s)	% Overshoot
Taguchi-GRA	0.0289	0.0042	3
MRAC	0.407	0.222	0
GA	0.032	0.006	20.1
PSO	0.031	0.005	19.4

6. Conclusions

An improved design of a multi-response optimized PID controller is presented by combining the Taguchi method with GRA in this work. The PID parameters K_p, K_i, and K_d, were selected to define the search space for the multi-objective optimization problem. The optimization objective was to minimize both T_s and $\% OS$ of the DC motor's speed. After Taguchi-GRA, the optimum PID parameter combination were obtained as: $K_p = 2.6$, $K_i = 228$, and $K_d = 0.008$. The ANOVA for GRG showed that P values for K_d and K_p are less than 0.05. Hence, K_d and K_p are considered the significant factors that affected T_s and $\% OS$. The step response using the Taguchi-GRA method demonstrated the superiority over the conventional ZN-tuned PID in terms of transient response.

The MRAC schemes using the MIT rule, Lyapunov rule, and modified MIT rule for DC motor speed control were evaluated and compared in this study. The work also highlighted the advantages of using the modified MIT rule and Lyapunov rule. The simulation results clearly showed that the modified MIT rule outperformed the conventional MIT rule when the reference input amplitude is changed. Unlike conventional controllers, the MRAC scheme could handle disturbance and parameter changes with excellent tracking performance. It is also observed that the Lyapunov rule can be used for non-linear systems and has a better transient response compared to the MIT rule. Hence, the modified MIT rule and Lyapunov rule can replace the conventional controllers in industrial applications where DC motors are used.

References

[1] Trong T.N., *The control structure for DC motor based on the flatness control*, International Journal of Power Electronics and Drive Systems, vol. 8, no. 4, pp. 1814–1821 (2017), DOI: 10.11591/ijpeds.v8.i4.pp1814–1821.

[2] Li Z., Xia C., *Speed control of brushless DC motor based on CMAC and PID controller*, Proceedings of the 6th IEEE World Congress on Intelligent Control and Automation, Dalian, China, pp. 6318–6322 (2016).

[3] Wang M.S., Chen S.C., Shih C.H., *Speed control of brushless DC motor by adaptive network-based fuzzy inference*, Microsystem Technologies, vol. 24, no. 1, pp. 33–39 (2018), DOI: 10.1007/s00542-016-3148-0.

[4] Templos-Santos J.L., Aguilar-Mejia O., Peralta-Sanchez E., Sosa-Cortez R., *Parameter tuning of PI control for speed regulation of a PMSM using bio-inspired algorithms*, Algorithms, vol. 12, no. 3, pp. 54–75 (2019), DOI: 10.3390/a12030054.

[5] John D.A., Sehgal S., Biswas K., *Hardware Implementation and Performance Study of Analog $PI^{\lambda}D^{\mu}$ Controllers on DC Motor*, Fractal and Fractional, vol. 4, no. 3, pp. 34–45 (2020), DOI: 10.3390/fractalfract4030034.

[6] Serradilla F., Cañas N., Naranjo J.E., *Optimization of the Energy Consumption of Electric Motors through Metaheuristics and PID Controllers*, Electronics, vol. 9, no. 11, pp. 1842–1858 (2020), DOI: 10.3390/electronics9111842.

[7] Hammoodi S.J., Flayyih K.S., Hamad A.R., *Design and implementation speed control system of DC motor based on PID control and matlab Simulink*, International Journal of Power Electronics and Drive Systems, vol. 11, no. 1, pp. 127–134 (2020), DOI: 10.11591/ijpeds.v11.i1.pp127-134.

[8] Zhang Y., An Y., Wang G., Kong X., *Multi motor neural PID relative coupling speed synchronous control*, Archives of Electrical Engineering, vol. 69, no. 1, pp. 69–88 (2020), DOI: 10.24425/aee.2020.131759.

[9] Wu H., Su W., Liu Z., *PID controllers: Design and tuning methods*, Proceedings of the 9th IEEE Conference on Industrial Electronics and Applications, Hangzhou, China, pp. 808–813 (2014).

[10] Sheel S., Gupta O., *New techniques of PID controller tuning of a DC motor-development of a toolbox*, MIT International Journal of Electrical and Instrumentation Engineering, vol. 2, no. 2, pp. 65–69 (2012).

[11] Kumar P., Raheja J., Narayan S., *Design of PID Controllers Using Multiobjective Optimization with GA and Weighted Sum Objective Function Method*, International Journal of Technical Research, vol. 2, no. 2, pp. 52–56 (2013).

[12] Chiha I., Liouane N., Borne P., *Tuning PID Controller using Multi-objective Ant Colony Optimization*, Applied Computational Intelligence and Soft Computing, Article ID 536326, 7 pages (2012), DOI: 10.1155/2012/536326.

[13] de Moura Oliveira P.B., Hedengren J.D., Pires E.J., *Swarm-Based Design of Proportional Integral and Derivative Controllers Using a Compromise Cost Function: An Arduino Temperature Laboratory Case Study*, Algorithms, vol. 13, no. 12, pp. 315–332 (2020), DOI: 10.3390/a13120315.

[14] Dewantoro G., *Multi-objective optimization scheme for PID-controlled DC motor*, International Journal of Power Electronics and Drive Systems, vol. 7, no. 3, pp. 31–38 (2016), DOI: 10.11591/ijpeds.v7.i3.pp734-742.

[15] Achuthamenon Sylajakumari P., Ramakrishnasamy R., Palaniappan G., *Taguchi Grey Relational Analysis for Multi-Response Optimization of Wear in Co-Continuous Composite*, Materials, vol. 11, no. 9, pp. 3–17 (2018), DOI: 10.3390/ma11091743.

[16] El-Samahy A.A., Shamseldin M.A., *Brushless DC motor tracking control using self-tuning fuzzy PID control and model reference adaptive control*, Ain Shams Engineering Journal, vol. 9, no. 3, pp. 341–352 (2018), DOI: 10.1016/j.asej.2016.02.004.

[17] Neogi B., Islam S.S., Chakraborty P., Barui S., Das A., *Introducing MIT rule toward the improvement of adaptive mechanical prosthetic arm control model*, In Progress in Intelligent Computing Techniques: Theory, Practice, and Applications, Springer, Singapore, pp. 379–388 (2018).

[18] Akbar M.A., Naniwa T., Taniai Y., *Model reference adaptive control for DC motor based on Simulink*, Proceeding of the 6th IEEE International Annual Engineering Seminar (InAES), Yogyakarta, Indonesia pp. 101–106 (2016).

[19] Sethi D., Kumar J., Khanna R., *Design of fractional order MRAPIDC for inverted pendulum system*, *Indian Journal of Science and Technology*, vol. 10, no. 31, pp. 1–5 (2017), DOI: 10.17485/ijst/2017/v10i31/113893.

[20] Jain P., Nigam M.J., *Design of a model reference adaptive controller using modified MIT rule for a second-order system*, Advances in Electronic and Electric Engineering, vol. 3, no. 4, pp. 477–484, (2013).

[21] Dimeas I., Petras I., Psychalinos C., *New analog implementation technique for fractional-order controller: a DC motor control*, AEU-International Journal of Electronics and Communications, vol. 78, pp. 192–200 (2017), DOI: 10.1016/j.aeue.2017.03.010.

[22] Qader M.R., *Identifying the optimal controller strategy for DC motors*, Archives of Electrical Engineering, vol. 68, no. 1, pp. 101–114 (2019), DOI: 10.11591/ijra.v6i4.pp252-268.

[23] George M.A., Kamath D.V., *OTA-C voltage-mode proportional- integral- derivative (PID) controller for DC motor speed control*, Proceedings of the Academicsera 461st International Conference on Science, Technology, Engineering and Management (ICSTEM), Paris, France, pp. 21–26 (2019).

[24] Swarnkar P., Jain S.K., Nema R.K., *Adaptive control schemes for improving the control system dynamics: a review*, IETE Technical Review, vol. 31, no. 1, pp. 17–33 (2014), DOI: 10.1080/02564602.2014.890838.

[25] Hägglund T., *The one-third rule for PI controller tuning*, Computers & Chemical Engineering, vol. 127, pp. 25–30 (2019), DOI: 10.1016/j.compchemeng.2019.03.027.

[26] George M.A., Kamath D.V., Thirunavukkarasu I., *An Optimized Fractional-Order PID (FOPID) Controller for a Non-Linear Conical Tank Level Process*, Proceedings of IEEE Applied Signal Processing Conference (ASPCON), Kolkata, India, pp. 134–138 (2020).